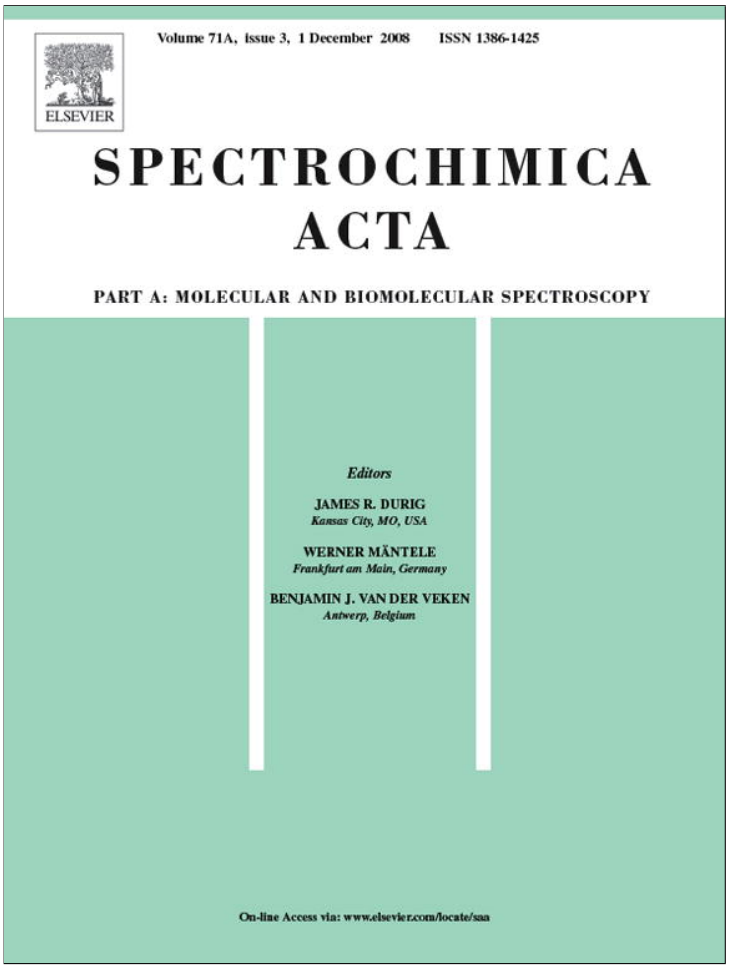

Spectrochimica Acta Part A 71 (2008) 969–974

Contents lists available at ScienceDirect

Spectrochimica Acta Part A: Molecular and Biomolecular Spectroscopy

journal homepage: www.elsevier.com/locate/saa

IR spectroscopic investigation of *cis*-$(CH_3)_2$Au(*O*,*O*′-acac) and *cis*-$(CD_3)_2$Au(*O*,*O*′-acac)

Miyako Hisamoto[a], Susannah L. Scott[a,b,*]

[a] *Department of Chemical Engineering, University of California, Santa Barbara, CA 93106-5080, USA*
[b] *Department of Chemistry, University of California, Santa Barbara, CA 93106-5080, USA*

ARTICLE INFO

Article history:
Received 13 November 2007
Received in revised form 5 February 2008
Accepted 13 February 2008

Keywords:
Gold(III)
Acetylacetonato complex
Vibrational spectrum
Density functional theory
Isotope labeling

ABSTRACT

The IR spectrum of *cis*-$(CH_3)_2$Au(*O*,*O*′-acac) has been reassigned by comparing frequencies for *cis*-$(CH_3)_2$Au(*O*,*O*′-acac) and *cis*-$(CD_3)_2$Au(*O*,*O*′-acac), and by analysis of the DFT-calculated normal modes and their frequencies for the isolated molecules. The vibrational intensity in the C–H stretching region arises almost entirely from the *cis*-$(CH_3)_2$Au fragment, while the methyl deformation intensity is largely of acetylacetonato ligand origin. A low frequency mode in the C–H stretching region is the first overtone of the $\delta_a(CH_3)$ mode of *cis*-$(CH_3)_2$Au. The Au–C stretching modes are affected by deuteration of the *cis*-$(CH_3)_2$Au fragment, while the Au–O stretching modes are not.

1. Introduction

Organogold compounds have long been used in therapeutic formulations [1], in laser-directed (LCVD) [2] and electron-beam-induced [3] chemical vapor deposition of gold spots and lines for electronics applications, in metal organic chemical vapor deposition (MOCVD) and chemical fluid deposition (CFD) [4] of thin gold films, as homogeneous catalysts for organic reactions [5] and in the preparation of supported gold catalysts by CVD [6–8]. Volatile *cis*-$(CH_3)_2$Au(*O*,*O*′-acac) [9] is the most widely-used compound for CVD (m.p. 82 °C, dec 180 °C), despite its air-, light- and temperature-sensitivity [2]. Its reaction chemistry has been reported in solution [10–12], in the gas phase [13] and on surfaces [14–19]. For oxide surfaces with low isoelectric points such as silicas and silica-aluminas, its use facilitates the synthesis of highly-dispersed gold nanoparticles [20,21], since conventional liquid-phase ion-exchange methods largely fail for these support materials [22].

Accurate spectroscopic assignments are essential for monitoring and interpreting the reactions of organometallic complexes in solution, and on surfaces. In particular, our understanding of the interaction of *cis*-$(CH_3)_2$Au(*O*,*O*′-acac) with a variety of oxide surfaces is predicated on spectroscopic (primarily IR) analysis of the compound before and after its deposition [17,19,23–25]. In this contribution, we present a detailed analysis of the IR spectrum of *cis*-$(CH_3)_2$Au(*O*,*O*′-acac). Since (acetylacetonato)metal complexes possess many strongly-mixed vibrational modes [26], we base our IR assignments on a combination of experimentally-observed isotope shifts, comparison with DFT-predicted frequencies, and examination of theoretical normal modes.

2. Experimental and computational methods

$(CH_3)_2$Au(acac) was purchased from Strem and used as received. It was stored in the dark at −35 °C and handled in an inert atmosphere, using glovebox and Schlenk techniques. $(CD_3)_2$Au(acac) was synthesized following literature methods [11,27], with ligroin (reagent grade, Aldrich), anhydrous pyridine (99.8%, Aldrich), ethylenediamine (99%, Alfa Aesar), methyl-d_3-magnesium iodide solution (1.0 M in diethyl ether, 99 atom% D, Aldrich) and thallium(I) acetylacetonate (97% min, Alfa Aesar) used as received. Its identity and isotopic purity were assessed by solution-state NMR [11]. KBr (SpectroGrade™, International Crystal Labs) and BN (>99%, Strem) were dried under vacuum before use and stored under N_2. $AuCl_3$ (Aldrich) and acetylacetone (ReagentPlus®, ≥99%, Aldrich) were used as received.

IR spectra were recorded on a Shimadzu Prestige IR spectrometer, equipped with a modified sample compartment to accommodate an air-free IR cell. The spectrometer was equipped with a DTGS detector and purged with CO_2-free dry air from a

* Corresponding author at: Department of Chemical Engineering, University of California, Santa Barbara, CA 93106-5080, USA. Tel.: +1 805 893 5606; fax: +1 805 893 4731.
E-mail address: sscott@engineering.ucsb.edu (S.L. Scott).

1386-1425/$ – see front matter © 2008 Elsevier B.V. All rights reserved.
doi:10.1016/j.saa.2008.02.020

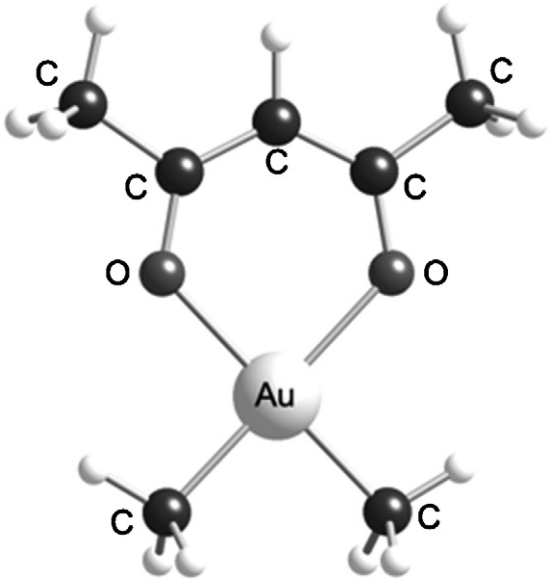

Fig. 1. DFT-calculated structure for an isolated molecule of *cis*-$(CH_3)_2$Au(*O,O′*-acac) [37].

Balston 75-52 Purge Gas Generator. Polycrystalline $(CH_3)_2$Au(acac) and $(CD_3)_2$Au(acac) were mixed with KBr and pressed into pellets under N_2. Each pellet was then placed in a sealed IR cell under an inert atmosphere while its spectrum was recorded. Spectra were recorded with 4 cm^{-1} resolution by averaging 50 scans.

Computations were performed using the DFT implementation in the Gaussian03 code, Revision C.02 [28]. Geometry optimizations were performed using the hybrid exchange functional B3LYP [29–31]. Au core electrons were treated by a pseudopotential using the standard LANL2 parameter set (electron–electron and nucleus–electron), while Au valence electrons were treated by an uncontracted basis set from LANL2DZ. The 6-31G(d′) basis set, in which correlation energies are extrapolated to the complete basis set limit, was used to describe all other atoms [32]. Stationary points were characterized by the calculation of vibrational frequencies, and the geometry was found to be a minimum energy structure ($N_{imag} = 0$). DFT methods tend to overestimate IR frequencies [33,34]. However, no attempt was made to improve the agreement with experimental frequencies by applying a global scaling factor, due to the need for different calibration factors to describe different types of vibrational modes [35]. Spectra were predicted by assigning a Lorentzian band profile with a half-width of 2 cm^{-1} to each IR-active mode.

3. Results and discussion

3.1. Computational modeling of $(CH_3)_2$Au(acac)

In order to provide a basis for assigning the IR spectrum of the polycrystalline material (see below), we investigated the vibrations of both *cis*-$(CH_3)_2$Au(*O,O′*-acac) and *cis*-$(CD_3)_2$Au(*O,O′*-acac) using the isolated molecule as a computational model, Fig. 1. Its bond distances (Au–C 2.047 Å; Au–O 2.141 Å) agree reasonably well with those measured by gas-phase electron diffraction (Au–C 2.054(5) Å; Au–O 2.085(7) Å) [36], although the calculated Au–O distance is slightly overestimated. In the solid-state, a crystal structure shows that the molecule has essentially the same structure but lacks a C_2 axis, with inequivalent Au–C and Au–O bonds [37].

The predicted IR frequencies and their normal mode assignments are reported in Tables 1–3. The vibrations of the undeuterated acetylacetonato ligand are virtually identical for both isotopologs, and are in good agreement with recent assignments for M(acac)$_3$ (M is Fe, Cr, Sc, Al) [38]. However, they differ substantially from the published assignments for $(CH_3)_2$Au(acac) [39], which were based on the normal coordinate analysis of Nakamoto [40]. Details of the assignments are described below. Calculated IR spectra are shown for different frequency regions of the IR spectra in Figs. 2–5.

Table 1
IR frequencies above 2000 cm^{-1} for polycrystalline *cis*-$(CH_3)_2$Au(*O,O′*-acac) and *cis*-$(CD_3)_2$Au(*O,O′*-acac),[a] with comparison to the frequencies of the DFT-predicted IR vibrations[b] and their assignments for the corresponding isolated molecules

$(CH_3)_2$Au(acac)		$(CD_3)_2$Au(acac)		Assignment[c]
Calculated	Observed	Calculated	Observed	
3217 (0.02)	n.d.	3217 (0.02)	n.d.	ν(CH), methine
3162 (0.03)	2984 m			$\nu_a(CH_3)$, $(CH_3)_2$Au
3160 (0.01)				
3159 (0.04)				
3154 (0.00)				
3152 (0.00)	n.d.	3152 (0.00)	2980 w,br	$\nu_a(CH_3)$, CCH_3
3151 (0.06)		3151 (0.06)		
3119 (0.03)		3119 (0.03)		
3118 (0.00)		3118 (0.00)		
3059 (0.05)	2911 m			$\nu_s(CH_3)$, $(CH_3)_2$Au
3056 (0.03)				
3054 (0.03)	n.d.	3054 (0.03)	2924 w	$\nu_s(CH_3)$, CCH_3
	2808 w			$2\delta_a(CH_3)$, $(CH_3)_2$Au
		2347 (0.02)	2239 m	$\nu_a(CD_3)$, $(CD_3)_2$Au
		2345 (0.01)		
		2343 (0.02)		
		2339 (0.00)		
		2188 (0.03)	2118 m	$\nu_s(CD_3)$, $(CD_3)_2$Au
		2186 (0.02)		
			2060 w	$2\delta_a(CD_3)$, $(CD_3)_2$Au

[a] Recorded as KBr disks.
[b] Unscaled. Calculated intensities shown in parentheses.
[c] Based on analysis of theoretical normal modes. Symbols: ν, stretching; δ, in-plane bending; n.d., not detected.

3.2. C–H/C–D stretching vibrations

The IR spectrum of polycrystalline *cis*-$(CH_3)_2$Au(*O,O′*-acac) in the C–H stretching region (3100–2800 cm^{-1}) is shown in Fig. 2a. The two most intense vibrations at 2984 and 2911 cm^{-1} are assigned to the antisymmetric and symmetric C–H stretching modes, respectively, of the *cis*-$(CH_3)_2$Au fragment, Table 1. In order to assess the contributions from C–H stretching in the acetylacetonato ligand, we recorded the spectrum of polycrystalline *cis*-$(CD_3)_2$Au(*O,O′*-acac). In the same spectral region, its vibrations are much weaker, Fig. 2b. The C–D stretching region of the partially deuterated compound is even clearer, Fig. 3b, with two peaks at 2239 and 2118 cm^{-1} that are readily assigned to antisymmetric and symmetric stretching modes, respectively, of *cis*-$(CD_3)_2$Au, and a third vibration at 2060 cm^{-1}. The IR intensities of the C–H stretching modes of the acetylacetonate ligand must therefore be much lower than those of the $(CH_3)_2$Au fragment, which we attribute to the higher polarity of AuC–H bonds compared to CC–H bonds. Curiously, the lower relative intensities of the acetylacetonate C–H stretches are not predicted in the DFT-calculated spectrum. The acetylacetonate methine stretch is also not detected experimentally, in spite of its significant calculated intensity.

The band at 2808 cm^{-1} must be a vibration of the *cis*-$(CH_3)_2$Au fragment, since a similar three-peak pattern is seen in both the C–H and C–D stretching regions of the two isotopologs. In a previous study [39], the peak at 2808 cm^{-1} was assigned to a $\nu_s(CH_3)$ vibration of the *cis*-$(CH_3)_2$Au fragment. It was suggested that the symmetric CH_3 stretching mode is split into in-phase and out-of-phase components (i.e., 2911 and 2808 cm^{-1}), by analogy to

Table 2
IR frequencies in the range 2000–1100 cm^{-1} for polycrystalline *cis*-$(CH_3)_2Au(O,O'$-acac) and *cis*-$(CD_3)_2Au(O,O'$-acac),[a] with comparison to the frequencies of the DFT-predicted IR vibrations[b] and their assignments for the corresponding isolated molecules

$(CH_3)_2Au$(acac)		$(CD_3)_2Au$(acac)		Assignment[c]
Calculated	Observed	Calculated	Observed	
1637 (1.00)	1595 s	1637 (1.00)	1598 s	ν_s(CO)
			1557 m	combination: $\delta_s(CD_3) + \pi(CD_3)$[d]
	1543 m		1535 m	2γ(CH)[d]
1569 (0.60)	1518 s	1569 (0.60)	1518 s	δ(CH) + ν_a(CCC)
1521 (0.02)	n.d.	1520 (0.02)	n.d.	$\delta_a(CH_3)$, CCH_3 + δ(CH) + ν_a(CO)
1501 (0.12)	1421 sh	1501 (0.12)	1421 sh	$\delta_a(CH_3)$, CCH_3
1496 (0.01)		1496 (0.01)		
1495 (0.00)		1495 (0.00)		
1495 (0.00)	n.d.			$\delta_a(CH_3)$, $(CH_3)_2Au$
1494 (0.02)				
1486 (0.00)				
1485 (0.00)				
1460 (0.39)	1391 s	1459 (0.37)	1391 s	ν_a(CO) + ν_a(CCC) + $\delta_a(CH_3)$, CCH_3
1418 (0.00) 1416 (0.02)	1352 s	1418 (0.00) 1416 (0.02)	1352 s	$\delta_s(CH_3)$, CCH_3
1308 (0.03)	1234 m			$\delta_s(CH_3)$, $(CH_3)_2Au$, in-phase
1289 (0.09)	1263 m	1289 (0.08)	1263 m	ν_s(CCC) + $\delta_s(CH_3)$, CCH_3
1272 (0.00)	1209 w			$\delta_s(CH_3)$, $(CH_3)_2Au$ out-of-phase + δ(CH)
1242 (0.04)	1196 m	1243 (0.03)	1204 m	δ(CH)

[a] Recorded as KBr disks.
[b] Unscaled. Calculated intensities shown in parentheses.
[c] Based on analysis of theoretical normal modes. For mixed modes, contributing vibrations are indicated with '+' (not to be construed as combination modes, except where noted). Symbols: ν, stretching; δ, in-plane bending; n.d., not detected.
[d] Tentative assignment, see Table 3 for fundamentals.

the splitting of the $\delta_s(CH_3)$ modes of the *cis*-$(CH_3)_2Au$ fragment (see below). However, DFT predicts a frequency difference for the $\nu_s(CH_3)$ modes of only 3 cm^{-1} for these modes in the isolated *cis*-$(CH_3)_2Au(O,O'$-acac) molecule.

In the absence of any DFT-predicted fundamentals near these frequencies, we reassign the bands at 2808 and 2060 cm^{-1} to the overtones $2\delta_a(CH_3)$ and $2\delta_a(CD_3)$ for the respective *cis*-$(CH_3)_2Au$ fragments. The IR spectra of $[$*cis*-$(CH_3)_2Au(\mu$-I$)]_2$ and

Table 3
IR frequencies below 1100 cm^{-1} for polycrystalline *cis*-$(CH_3)_2Au(O,O'$-acac) and *cis*-$(CD_3)_2Au(O,O'$-acac),[a] with comparison to the frequencies of the DFT-predicted IR vibrations[b] and their assignments for the corresponding isolated molecules

$(CH_3)_2Au$(acac)		$(CD_3)_2Au$(acac)		Assignment[c]
Calculated	Observed	Calculated	Observed	
		1085 (0.01) 1084 (0.00)	1042	$\delta_a(CD_3)$, $(CD_3)_2Au$
		1078 (0.00)		
		1076 (0.00)		
1069 (0.00)	1022 s,br	1069 (0.00)	1022 s	$\pi(CH_3)$, CCH_3
1054 (0.03) 1052 (0.04)		1054 (0.03) 1052 (0.03)		
1049 (0.00)		1050 (0.00)		
		1005 (0.02)	955 m	$\delta_s(CD_3)$, $(CD_3)_2Au$, in-phase
		982 (0.02)	941 m	$\delta_s(CD_3)$, $(CD_3)_2Au$, out-of-phase
956 (0.02)	928 m	955 (0.01)	928 m	ν_a(C–CH_3)
954 (0.02)	928 m	953 (0.02)	928 m	ν_s(C–C–C) + $\rho(CH_3)$, CCH_3
911 (0.00)	831 w			$\rho(CH_3)$, $(CH_3)_2Au$
896 (0.00)				
888 (0.00)	831 w			$\pi(CH_3)$, $(CH_3)_2Au$
872 (0.02)				
803 (0.02)	777 s	803 (0.02)	781 s	γ(CH)
		688 (0.02)	n.d.	$\rho(CD_3)$, $(CD_3)_2Au$
680 (0.01)	687 m	682 (0.02)	687 m	$\pi(CH_3)$, CCH_3
		681 (0.01)	n.d.	$\rho(CD_3)$, $(CD_3)_2Au$ + $\rho(CH_3)$, CCH_3
678 (0.03)	648 m			Δ + ν_s(C–CH_3)
		676 (0.02)	652 m	$\rho(CD_3)$, $(CD_3)_2Au$ + Δ
		666 (0.00)	621 w	$\pi(CD_3)$, $(CD_3)_2Au$
		653 (0.01)		
602 (0.05)	610 m	597 (0.05)	604 m	Δ
578 (0.00)	583 w			$\nu_s(AuC_2)$
570 (0.00)	n.d.	570 (0.00)	n.d.	$\rho(CH_3)$, CCH_3 + Γ
565 (0.01)	573 w			$\nu_a(AuC_2)$
		529 (0.01)	532 w	$\nu_s(AuC_2)$
		519 (0.00)	n.d.	$\nu_a(AuC_2)$
439 (0.05)	442 s	439 (0.05)	444 s	$\nu_s(AuO_2)$
429 (0.00)	426 m	428 (0.00)	424 m	$\nu_a(AuO_2)$

[a] Recorded as KBr disks.
[b] Unscaled. Calculated intensities shown in parentheses.
[c] Based on analysis of theoretical normal modes. For mixed modes, contributing vibrations are indicated with '+'. Symbols: ν, stretching; δ, in-plane bending; γ, out-of-plane bending; ρ, rocking in-plane; π, rocking out-of-plane; Δ, in-plane ring deformation; Γ, out-of-plane ring deformation; n.d., not detected.

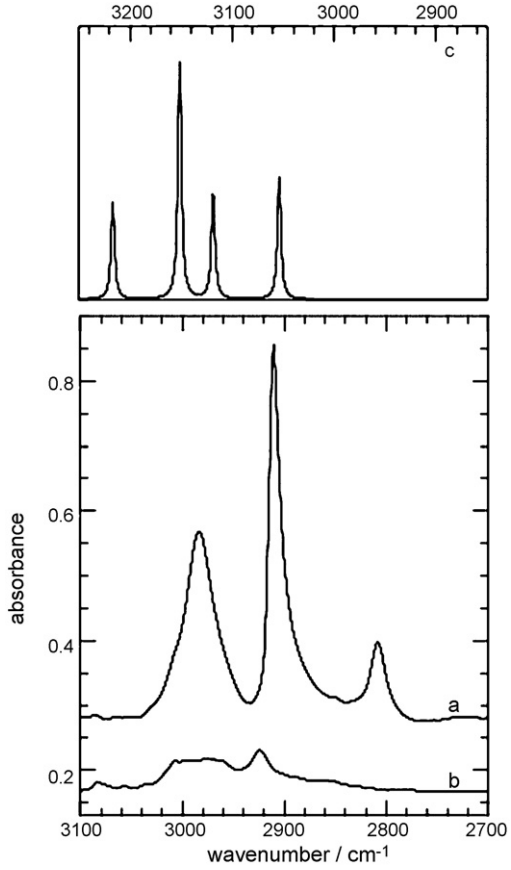

Fig. 2. Transmission IR spectra of (a) polycrystalline *cis*-$(CH_3)_2Au(O,O'$-acac); (b) polycrystalline *cis*-$(CD_3)_2Au(O,O'$-acac); and (c) calculated IR spectrum of *cis*-$(CH_3)_2Au(O,O'$-acac), in the region of the C–H stretching vibrations. Spectra (a) and (b) are vertically offset; spectrum (c) is offset horizontally.

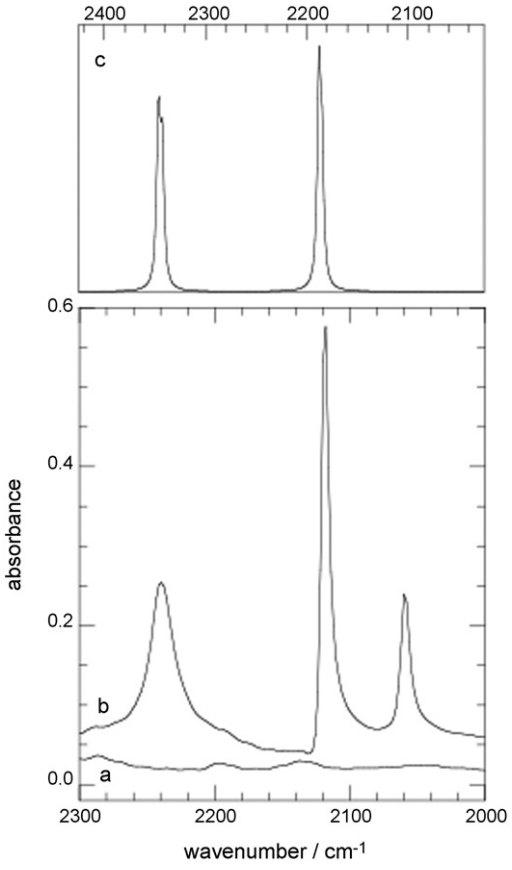

Fig. 3. Transmission IR spectra of (a) polycrystalline *cis*-$(CH_3)_2Au(O,O'$-acac); (b) polycrystalline *cis*-$(CD_3)_2Au(O,O'$-acac); and (c) calculated IR spectrum of *cis*-$(CD_3)_2Au(O,O'$-acac), in the region of the C–D stretching vibrations. Spectra (a) and (b) are vertically offset; spectrum (c) is offset horizontally.

[*cis*-$(CH_3)_2AuX_2^-$] (X is Cl, Br) also show three-peak patterns in their C–H stretching regions, and the lowest frequency band has been assigned to $2\delta_a(CH_3)$ [41]. Although the $\delta_a(CH_3)$ fundamental for *cis*-$Au(CH_3)_2$, expected at ca. 1400 cm^{-1}, is obscured by an intense band at 1392 cm^{-1} (see below), the position of the $\delta_a(CD_3)$ fundamental, clearly observed at 1042 cm^{-1}, is consistent with this assignment. The frequencies of the deformation overtones are slightly reduced and their intensities enhanced by Fermi resonance with the $\nu_s(CH_3)$ and $\nu_s(CD_3)$ modes of *cis*-$Au(CH_3)_2$ [42].

3.3. Vibrations of the acetylacetonate ring

The region from 1800 to 1100 cm^{-1} contains strongly-coupled C–O and C–C stretching modes, as well as the CH_3 and CH deformations. Bands associated with the acetylacetonate ring were attributed by comparison to the DFT-calculated frequencies in Table 2, with assignments for the deformations of the different kinds of methyl groups aided by comparison of the spectra for *cis*-$(CH_3)_2Au(O,O'$-acac) and *cis*-$(CD_3)_2Au(O,O'$-acac). Our assignments differ from those reported for *cis*-$(CH_3)_2Au(O,O'$-acac) on the basis of normal coordinate analysis [39]. The two most intense vibrations, at 1595 and 1518 cm^{-1}, are the symmetric CO stretch and the methine in-plane bend mixed with the antisymmetric C–C–C stretch of the acetylacetonate backbone, respectively. No fundamentals are predicted to appear between them. Therefore we propose the assignment of the peak observed at 1543 cm^{-1} to the first overtone $2\gamma(CH)$ (expected $2 \times 777 = 1554$ cm^{-1}). The peak at 1557 cm^{-1} is observed only for *cis*-$(CD_3)_2Au(O,O'$-acac), and is assigned to the combination $\delta_s(CD_3) + \pi(CD_3)$ (expected 955/941 + 621 = 1576/1562 cm^{-1}).

The antisymmetric CO stretch, at 1391 cm^{-1}, is mixed with the antisymmetric C–C–C stretch and the antisymmetric deformation of the acetylacetonate methyl groups, while the symmetric C–C–C stretch is mixed with the symmetric deformation of the acetylacetonate methyl groups, and appears at 1263 cm^{-1}. The former obscures the $\delta_a(CH_3)$ mode of the *cis*-$(CH_3)_2Au$ fragment. The $\delta_s(CH_3)$ mode for the *cis*-$(CH_3)_2Au$ fragment appears at a lower frequency than the $\nu_s(CCC)$ mode, even though its calculated frequency is higher, due to greater anharmonicity in the vibration involving C–H bonds. The $\delta_s(CH_3)$ mode is further split into in-phase and out-of-phase components (1234/1209 cm^{-1}), with the magnitude of the splitting comparable to that predicted by DFT. Finally, methine in-plane bending appears at 1196 cm^{-1}.

In contrast to the relative intensities of the C–H stretching modes for the two kinds of methyl groups, the intensities of the methyl deformations are much weaker for the *cis*-$(CH_3)_2Au$ fragment than for the acetylacetonate ligand. Consequently, deuteration in the *cis*-$(CD_3)_2Au$ fragment results in almost no change in this region of the spectrum, with the exception of the absent $\delta_s(CH_3)$ modes for the *cis*-$(CH_3)_2Au$ fragment (1234/1209 cm^{-1}). Again, the intensity difference for the vibrations of the two types of methyl groups is not predicted in the DFT calculations.

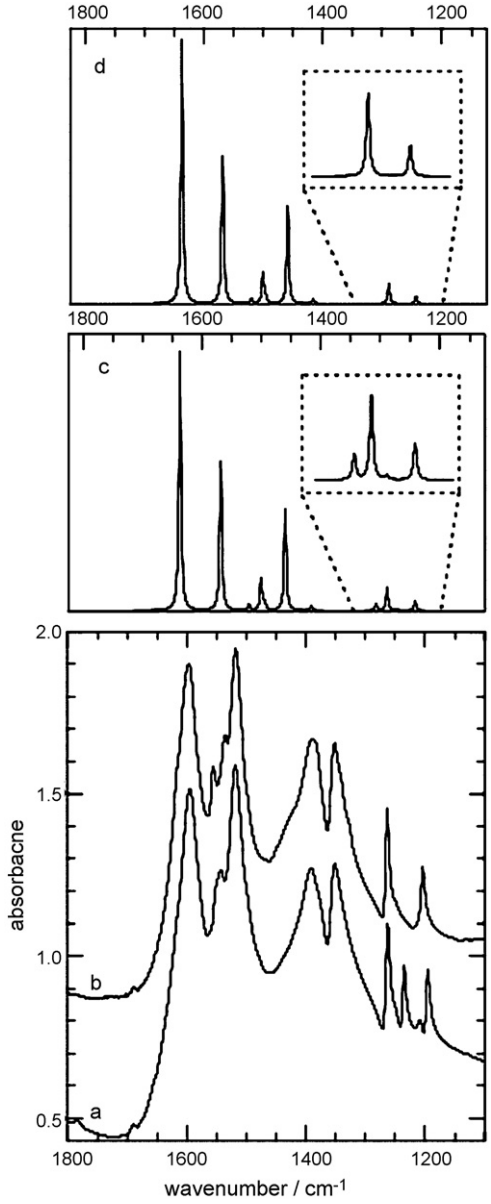

Fig. 4. Transmission IR spectra of (a) polycrystalline *cis*-$(CH_3)_2$Au(*O,O′*-acac); (b) polycrystalline *cis*-$(CD_3)_2$Au(*O,O′*-acac); and calculated IR spectra of (c) *cis*-$(CH_3)_2$Au(*O,O′*-acac); (d) *cis*-$(CD_3)_2$Au(*O,O′*-acac), in the region of the acetylacetonate ring vibrations. Spectra (a) and (b) are vertically offset; spectra (c) and (d) are offset horizontally.

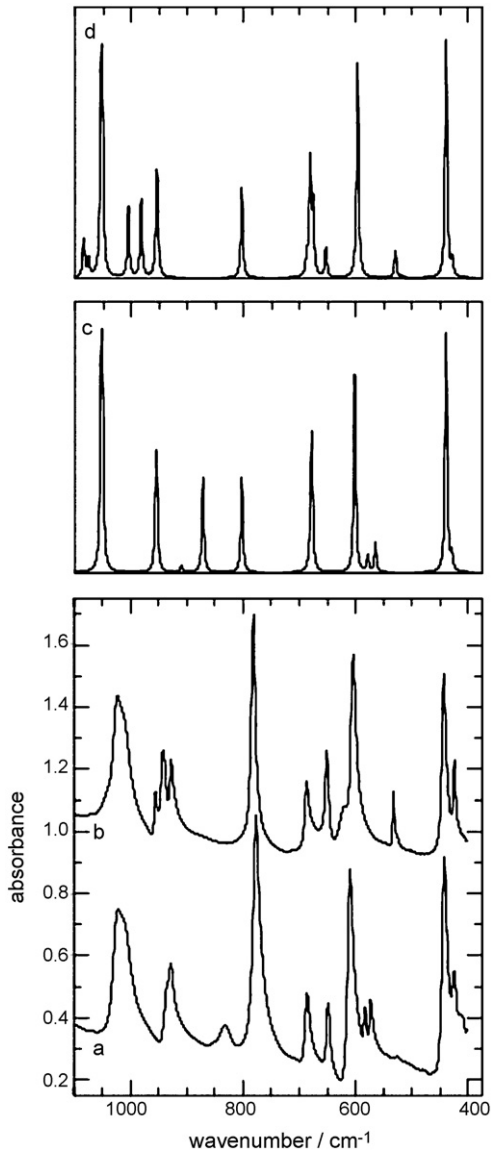

Fig. 5. Transmission IR spectra of (a) polycrystalline *cis*-$(CH_3)_2$Au(*O,O′*-acac); (b) polycrystalline *cis*-$(CD_3)_2$Au(*O,O′*-acac); and calculated IR spectra of (c) *cis*-$(CH_3)_2$Au(*O,O′*-acac); (d) *cis*-$(CD_3)_2$Au(*O,O′*-acac), in the fingerprint region. Spectra (a) and (b) are vertically offset.

3.4. Fingerprint region

In the region below 1100 cm^{-1}, the methyl rocking and torsion modes appear, as well as the Au–O and Au–C stretching vibrations. Deformations of the *cis*-$(CD_3)_2$Au fragment are red-shifted into this region. The $\delta_a(CD_3)$ mode of the *cis*-$(CD_3)_2$Au fragment is a shoulder on a broad band at 1022 cm^{-1} that contains the out-of-plane rocking modes of the acetylacetonate methyl groups. The pair of $\delta_s(CD_3)$ modes is seen clearly at 955/941 cm^{-1}. In-plane (Au)CH_3 rocking occurs at 831 cm^{-1}, red-shifted to 621 cm^{-1} for (Au)CD_3. The band at 928 cm^{-1} is assigned to C–CH_3 stretching of the acetylacetonate ligand, while the out-of-plane methine bend appears at 777 cm^{-1}.

The peaks at 648 and 610 cm^{-1} are ring deformations. The AuC_2 stretching modes appear as a pair of bands (symmetric and antisymmetric), at 583/573 cm^{-1} for *cis*-$(CH_3)_2$Au, while only a single band at 532 cm^{-1} is resolved for *cis*-$(CD_3)_2$Au. The large splitting for this mode in the spectrum of the undeuterated isotopolog, the isotope shift and the very small splitting in the spectrum of the deuterated isotopolog are predicted by DFT. In contrast, the symmetric and antisymmetric AuO_2 stretching modes, which appear at 442/426 cm^{-1}, are expected and observed to be virtually unaffected by deuterium labeling in these methyl groups.

4. Conclusions

The IR spectrum of *cis*-$(CH_3)_2$Au(*O,O′*-acac) has been completely reassigned, using the DFT-predicted frequencies and assignments of the theoretical normal modes, as well as partial isotopic labeling, as guides. The vibrations visible in the C–H stretching region are almost entirely due to the *cis*-$(CH_3)_2$Au fragment, while the methyl deformations are largely of acetylacetonate ligand origin. A low fre-

quency mode in the C–H stretching region is the first overtone of the $\delta_a(CH_3)$ mode of *cis*-$(CH_3)_2$Au. The intense acetylacetonato ring modes are strongly mixed. Au–C stretching is strongly affected by deuteration of the *cis*-$(CH_3)_2$Au fragment, while Au–O stretching is not.

Acknowledgement

This work was funded by the U.S. Department of Energy, Basic Energy Sciences, Catalysis Science Grant No. DE-FG02-03ER15467.

References

[1] C.F. Shaw III, Chem. Rev. 99 (1999) 2589.
[2] T.H. Baum, C.R. Jones, Appl. Phys. Lett. 47 (1985) 538.
[3] G. Xie, M. Song, K. Mitsuishi, K. Furuya, Appl. Surf. Sci. 241 (2005) 91.
[4] A. Cabañas, D.P. Long, J.J. Watkins, Chem. Mater. 16 (2004) 2028.
[5] A.S.K. Hashmi, Chem. Rev. 107 (2007) 3180.
[6] M. Okumura, S. Tsubota, M. Haruta, J. Mol. Catal. A: Chem. 199 (2003) 73.
[7] J. Guzman, B.C. Gates, Dalton Trans. (2003) 3303.
[8] G. Jacobs, S. Ricote, P.M. Patterson, U.M. Graham, A. Dozier, S. Khalid, E. Rhodus, B.H. Davis, Appl. Catal. A: Gen. 292 (2005) 229.
[9] F.H. Brain, C.S. Gibson, J. Chem. Soc. (1939) 762.
[10] G.E. Glass, R.S. Tobias, J. Organomet. Chem. 15 (1968) 481.
[11] R.B. Klassen, T.H. Baum, Organometallics 8 (1989) 2477.
[12] S. Komiya, J.K. Kochi, J. Am. Chem. Soc. 99 (1977) 3695.
[13] P.P. Semyannikov, G.I. Zharkova, V.M. Grankin, N.M. Tyukalevskaya, I.K. Igumenov, Metalloorg. Khim. 1 (1988) 1105.
[14] P.P. Semyannikov, V.M. Grankin, I.K. Igumenov, G.I. Zharkova, J. Phys. IV C5 (1995) 213.
[15] M. Okumura, K. Tanaka, A. Ueda, M. Haruta, Solid State Ionics 95 (1997) 143.
[16] M. Okumura, S.-I. Nakamura, S. Tsubota, T. Nakamura, M. Azuma, M. Haruta, Catal. Lett. 51 (1998) 53.
[17] J. Guzman, B.C. Gates, Langmuir 19 (2003) 3897.
[18] J. Guzman, S. Kuba, J.C. Fierro-Gonzalez, B.C. Gates, Catal. Lett. 95 (2004) 77.
[19] J. Guzman, B.G. Anderson, C.P. Vinod, K. Ramesh, J.W. Niemantsverdriet, B.C. Gates, Langmuir 21 (2005) 3675.
[20] M. Okumura, S.-I. Nakamura, S. Tsubota, T. Nakamura, M. Haruta, Prep. Catal. VII (1998) 277.
[21] A.K. Sinha, S. Seelan, S. Tsubota, M. Haruta, Stud. Surf. Sci. Catal. 143 (2002) 167.
[22] M. Haruta, Cattech 6 (2002) 102.
[23] J.C. Fierro-Gonzalez, V.A. Bhirud, B.C. Gates, Chem. Commun. (2005) 5275.
[24] J.C. Fierro-Gonzalez, B.C. Gates, Langmuir 21 (2005) 5693.
[25] V. Aguilar-Guerrero, B.C. Gates, Chem. Commun. (2007) 3210.
[26] D.A. Thornton, Coord. Chem. Rev. 104 (1990) 173.
[27] C.S. Gibson, W.M. Colles, J. Chem. Soc. 2407–2416 (1931).
[28] M.J. Frisch, G.W. Trucks, H.B. Schlegel, G.E. Scuseri, M.A. Robb, J.R. Cheeseman, J.J.A. Montgomery, T. Vreven, K.N. Kudin, J.C. Burant, J.M. Millam, S.S. Iyengar, J. Tomasi, V. Barone, B. Mennucci, M. Cossi, G. Scalmani, N. Rega, G.A. Petersson, H. Nakatsuji, M. Hada, M. Ehara, K. Toyota, R. Fukuda, J. Hasegawa, M. Ishida, T. Nakajima, Y. Honda, O. Kitao, H. Nakai, M. Klene, X. Li, J.E. Knox, H.P. Hratchian, J.B. Cross, V. Bakken, C. Adamo, J. Jaramillo, R. Gomperts, R.E. Stratmann, O. Yazyev, A.J. Austin, R. Cammi, C. Pomelli, J.W. Ochterski, P.Y. Ayala, K. Morokuma, G.A. Voth, P. Salvador, J.J. Dannenberg, V.G. Zakrzewski, S. Dapprich, A.D. Daniels, M.C. Strain, O. Farkas, D.K. Malick, A.D. Rabuck, K. Raghavachari, J.B. Foresman, J.V. Ortiz, Q. Cui, A.G. Baboul, S. Clifford, J. Cioslowski, B.B. Stefanov, G. Liu, A. Liashenko, P. Piskorz, I. Komaromi, R.L. Martin, D.J. Fox, T. Keith, M.A. Al-Laham, C.Y. Peng, A. Nanayakkara, M. Challacombe, P.M.W. Gill, B. Johnson, W. Chen, M.W. Wong, C. Gonzalez, J.A. Pople, Gaussian 03 Revision C. 02, Gaussian, Inc., Wallingford, CT, 2004.
[29] A.D. Becke, Phys. Rev. A 38 (1988) 3098.
[30] C. Lee, W. Yang, R.G. Parr, Phys. Rev. B 37 (1988) 785.
[31] B. Miehlich, A. Savin, H. Stoll, H. Preuss, Chem. Phys. Lett. 157 (1989) 200.
[32] G.A. Petersson, T.G. Tensfeldt, J.A. Montgomery Jr., J. Chem. Phys. 94 (1991) 6091.
[33] J. Florián, B.G. Johnson, J. Phys. Chem. 98 (1994) 3681.
[34] M.W. Wong, Chem. Phys. Lett. 256 (1996) 391.
[35] J. Baker, A.A. Jarzecki, P. Pulay, J. Phys. Chem. A 102 (1998) 1412.
[36] S. Shibata, K. Iijima, J. Chem. Soc., Dalton Trans. (1990) 1519.
[37] M. Hisamoto, S. Chattopadhyay, J. Eckert, G. Wu, S.L. Scott, submitted for publication, CCDC 666969.
[38] I. Diaz-Acosta, J. Baker, W. Cordes, P. Pulay, J. Phys. Chem. A 195 (2001) 238.
[39] M.G. Miles, G.E. Glass, R.S. Tobias, J. Am. Chem. Soc. 88 (1966) 5738.
[40] K. Nakamoto, Infrared and Raman Spectra of Inorganic and Coordination Compounds, 5th ed., Wiley, New York, 1997.
[41] W.M. Scovell, G.C. Stocco, R.S. Tobias, Inorg. Chem. 9 (1970) 2682.
[42] J.C. Lavalley, N. Sheppard, Spectrochim. Acta A 28 (1972) 2091.